JOURNAL OF MATERIALS SCIENCE 39 (2004) 5779–5784

Electroplating of zirconium and aluminum hydroxide thin films following anodic dissolution of corresponding metal anodes in organic medium

K. KAMADA, M. MUKAI, Y. MATSUMOTO
Department of Applied Chemistry and Biochemistry, Faculty of Engineering, Kumamoto University, 2-39-1 Kurokami, Kumamoto 860-8555, Japan
E-mail: kamada@chem.kumamoto-u.ac.jp

Zirconium (IV) hydroxide or hydrate oxide films, which are typically difficult to prepare by electrochemical methods using aqueous solutions, are easily fabricated in an acetone bath using Zr anodes as the metal sources and a metal-free solvent containing halide ions as the supporting electrolyte. This method is also confirmed to be applicable to aluminum anodes. In the early stage of electrolysis, anodic oxidation of the metal anode proceeds in the presence of water as an impurity in the solvent. Subsequently, pitting corrosion of the oxide film on the metal anode occurs as a result of the action of halide ions. The corrosiveness of the halogen additive appears to be an important factor determining the dissolution or deposition of metal species in this stage. That is, Br^- is more active for electrochemical dissolution of a passive oxide film on the anode compared to I^-. Finally, Zr species are deposited on the cathode surface via reactions with cathodically generated hydroxide ions. In these processes, the metal plate acts as a soluble anode and as a metal source for electrodeposition. The coating of Zr (IV) hydroxide film on a stainless steel substrate is shown to act as an effective barrier against electrolytic corrosion.

1. Introduction

The anodic dissolution of refractory metals (Al, Ti, Si, etc.) has recently been recognized as a new route for the fabrication of advanced inorganic materials. Two approaches have been proposed. One involves the fabrication of passive oxide films with unique structures on the metal surface after anodic dissolution [1, 2]. In particular, the selective dissolution of Al_2O_3 film on Al provides the nano-pore arrays, and such films are widely used as molecular membranes, templates for nano-sized materials [3, 4], and substrates with high specific surface area for fixing catalysts [5, 6]. Recently, Sugiura and coworkers reported that anodic polarization of polycrystalline TiO_2 in H_2SO_4 aqueous solution under ultraviolet irradiation resulted in the selective etching of bulk crystal to afford skeleton structures consisting of grain boundaries [7]. The other approach involves the fabrication of inorganic functional materials by reduction of dissolved metal ions generated through anodic dissolution of metals. Electrochemical synthesis of nano-sized metal clusters from a soluble metal anode in acetonitrile containing tetraoctylammonium salts serving as the supporting electrolyte has been proposed [8, 9]. In this method, metal cations dissolved from the anode are cathodically reduced, and the resultant aggregates of metal particles are stabilized by tetraoctylammonium cationic surfactants. Anodic electroplating of metal nitrides (MN_x) using a corresponding soluble metal anode (M) [10] can be easily carried out in a liquid-NH_3 medium [11], but such aqueous solutions are difficult to prepare.

The present authors have recently reported a new electrochemical method for the preparation of TiO_2 thin films, a refractory metal oxide, based on the use of a soluble titanium anode as a metal source in organic solutions with conductive additives [12]. In this method, anodic oxidation of the titanium anode occurs in the initial stage of electrolysis. TiO^{2+} is subsequently produced through dissolution of the oxide films and is electrodeposited directly onto the cathode surface. TiO^{2+} cations, which immediately undergo hydrolysis to form insoluble hydroxides or hydrated oxides in aqueous environments, can be readily stabilized in organic solvent.

In this contribution, the technique is extended to the synthesis of zirconia (ZrO_2) and alumina (Al_2O_3) thin films. Oxo-metal ions produced as a result of electrochemical dissolution of Al or Zr anode, are directly deposited onto the cathode surface as metal hydroxide. Finally, deposited films are converted into the oxide forms by dehydration and crystallization at elevated temperature. Alumina and zirconia thin films have a number of applications from an industrial point of view,

including surface insulation (chemical and electrical) of various metal substrates [13], catalysts, sensors [14], and electrolytes for solid oxide fuel cells (SOFC) [15]. In the conventional aqueous electrolysis system for fabrication of these films, however, the use of a soluble metal salt and control of the solution environment (pH and/or atmosphere) are required to stabilize the metal ions in solution [16, 17]. In contrast, the solutions used in the technique proposed here do not contain metal compounds at the start of electrolysis, thereby eliminating the need to find suitable soluble metal compounds.

2. Experimental

All electrodeposition experiments were performed in a two-electrode cell with undivided anodic and cathodic space as shown schematically in Fig. 1. Polycrystalline aluminum and zirconium foils (10×10 mm^2, thickness 0.15 mm) were used as the soluble anode, and platinum foil and stainless steel (10×10 mm^2, thickness 0.10 mm) were used as the cathode. The backs of electrodes were covered with insulating tape to prevent the development of an inhomogeneous potential distribution during electrolysis. The anode and cathode were set parallel at an opposing distance of 5 mm. The supporting electrolyte was 0.01 M I_2 or Br_2 in acetone solvent, and the as-received acetone reagent used in this study contained a small amount of water as an impurity (about 0.13 M). Electrolysis was carried out by applying a constant current or voltage using a DC power supply at room temperature. After electrolysis, the morphology and elemental distribution of the deposited films were observed by scanning electron microscopy (SEM; JSM-5310/LV, Jeol) and electron probe microanalysis (EPMA; JXA-8900, Jeol), and the crystal structure before and after heat treatment was analyzed based on X-ray diffraction (XRD) patterns (RINT-2500V, Rigaku; Cu-K_α radiation). Thermal analysis of cathodic deposits was performed by TG/DTA (TG/DTA 300, Seiko). The compositions of the deposited film and the solvent after electrolysis were analyzed by inductively coupled plasma (ICP) spectrophotometry (IRIS Advantage, Nippon Jarrell Ash). ICP analysis was carried out after evaporating off the solvent by dissolving the films and the residue in 2 M HCl solution to determine the amount of Al or Zr. The corrosive potential and current of stainless steel covered with the film after thermal treatment at 773 K were evaluated through measurement of potentiodynamic current-potential curves in 0.1 M KCl solution. A Pt plate and an Ag/AgCl (sat. KCl) electrode were employed as the counter and reference electrodes, respectively. The exposed area of the working electrode was 0.25 cm^2. All potentials were recorded at room temperature ($\sim$293 K). The potential was controlled using a potentiostat and was varied from -1.0 V to positive potentials at a scan rate of 1 mV/s.

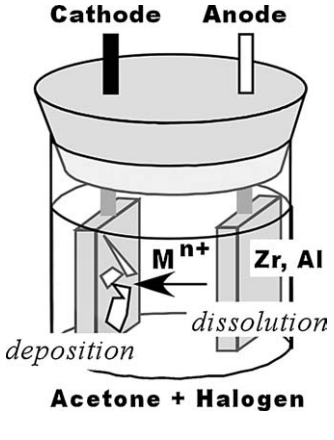

Figure 1 Schematic model of anodic dissolution of metal plate and subsequent cathodic deposition by the proposed technique.

3. Results and discussion

After electrolysis under a constant applied current of 5 mA for 10 min using the Zr anode, gel-like translucent thin films were produced on the cathode surface in acetone baths containing I_2 or Br_2 (abbreviated I-ACE and Br-ACE). The presence of Zr, O, and a trace amount of halogen was identified in the film by qualitative EPMA analysis, where the halogen impurities disappeared after thermal treatment above 773 K. As the solvent does not include a metal source, this result suggests that metal ions released from the anode deposit directly onto the cathode surface. Films containing Al and O were obtained in a similar manner using the Al anode. Therefore, in addition to Ti, Nb, and Ta [18], which have already been demonstrated as being feasibility for deposition by this process, Zr and Al films can also be electrodeposited by a simple electrochemical process. In this process, a metal plate acts as a soluble anode and a metal source for electrodeposition. Similar deposition will occur for transition-metal anodes such as Zn and Fe instead of refractory metals (Al, Zr, and Ti etc.) in an acetone bath containing a halogen. In this case, metal ions are integrated onto the cathode as the metal or a hydroxide depending on the specific chemical behavior.

Stefanov *et al*. [19] mentioned that the fabrication of zirconia thin films in aqueous system is problematic from an electrochemical point of view. That is, the hydrolysis of zirconium salts in aqueous solutions proceeds rapidly, and results in the production of the polymeric chains of zirconium hydroxide in all solutions. This rapid process leads to weak adhesion to the substrate. To resolve this problem it is necessary to maintain acidic conditions to stabilize the electrolyte during electrolysis, and pretreat the substrate to strengthen adhesion. In contrast, refractory aluminum species will dissolve in aqueous solutions over a wide range of pH as an ionic state (Al^{3+} under acidic conditions and $Al(OH)_4^-$ or AlO_2^- under alkaline conditions). For this reason, there have been many studies on the electrochemical synthesis of alumina thin films in aqueous solutions containing aluminum salts [13, 14]. As the technique proposed here has a number of advantages for the preparation of zirconia films as opposed to alumina films, the mechanism of electrolysis for Zr deposition is investigated below in detail.

Fig. 2 shows the typical evolution of applied voltage under a constant applied current of 5 mA using the

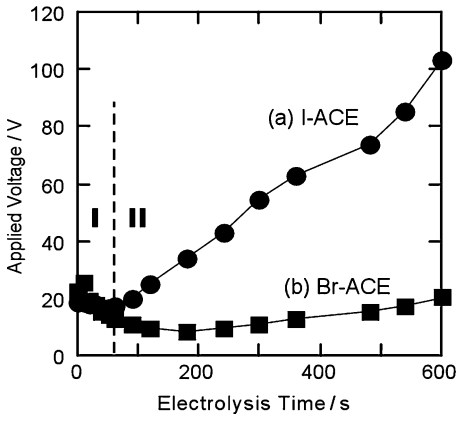

Figure 2 Applied voltage change in (a) I-ACE and (b) Br-ACE baths as a function of electrolysis time under a constant applied current of 5 mA.

Zr anode in I-ACE and Br-ACE. The applied voltages were roughly constant in the early period of electrolysis (<1 min; stage I), and then increased gradually with time (stage II). This behavior is comparable to the anodic oxidation of zirconium substrate under galvanostatic conditions [20]. In general, the anodic behavior of refractory metals is a competitive process between anodic oxidation due to growth of the passive film and electrochemical dissolution of the oxide film or anode. Anodic oxidation in this case is described by

$$Zr + 2H_2O \rightarrow ZrO_2 + 4H^+ + 4e^- \quad (1)$$

The halogen additive does not take part in the growth of the anodic oxide film. As the applied voltages in stage I are largely independent of the kind of additive, this process described by Equation 1 occurs preferentially in this stage. However, in stage II, the applied voltages differ remarkably between I-ACE and Br-ACE. This is due to the difference in corrosiveness of the halogen additive, with the result that Br-ACE exhibits lower voltage, representing more aggressive dissolution of the Zr anode compared to I-ACE.

Fig. 3 shows an SEM image of the surface of the Zr anode after potentiostatic electrolysis at 50 V for 10 min in Br-ACE. The surface became tarnished and blackish with appreciably pitting as a result of selective dissolution (pitting corrosion). In general, the development of spatial variation in electrical conductivity of the anodic oxide films results in local dissolution (pitting corrosion) at sites of relatively high conductivity. The observed voltage change is consistent with a process in which the formation rate of the passive film is initially higher than the dissolution rate, but gradually decreasing over time such that the dissolution rate becomes predominant [21].

Fig. 4 shows the variation in the amounts of Zr in the solvent and as-deposited film after galvanostatic electrolysis under 5 mA as a function of time, as determined by ICP analysis. The amount of Zr in the solvent and cathodic film increase linearly with electrolysis time, independent of the kind of additive, suggesting that the deposition amount, reflecting the film thickness, can be easily manipulated by the electrolysis time. The Zr contents of the solvent and film prepared in Br-ACE were higher than those prepared in I-ACE in all cases, consistent with the expectation regarding the corrosiveness of the halogenated bath. Commonly, the addition of halogen molecules (X_2) to acetone solvents results in the production of proton and halide ions by the following H_2O-catalyzed reaction [22].

$$CH_3COCH_3 \leftrightarrow CH_3C(OH)CH_2 \rightarrow CH_3COCH_2X + H^+ + X^- \quad (2)$$

In addition, the reaction of halogen molecules with H_2O also results in the production of H^+ and X^-. Thus, protons and halide ions (X^-) will present in the solvent and will play a role as supporting electrolytes during electrolysis, as evidenced by the lack of anodic

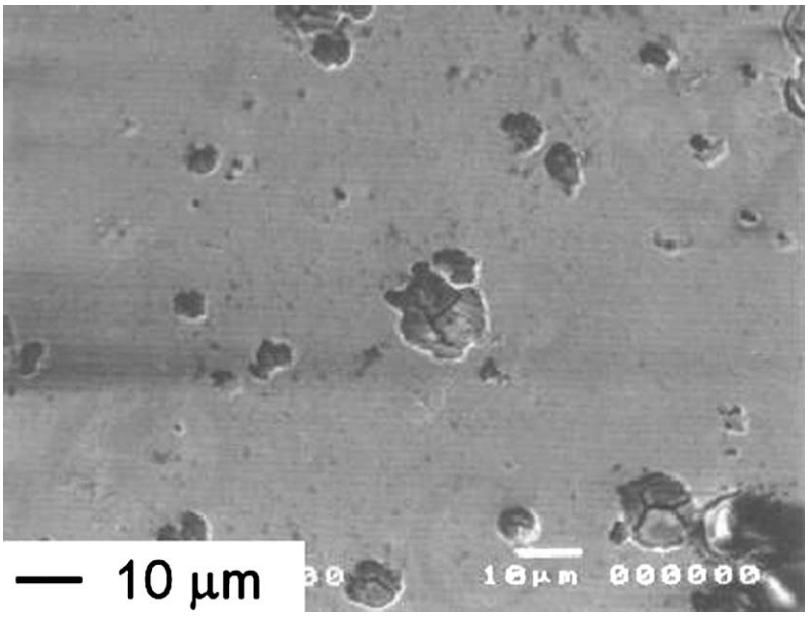

Figure 3 SEM images of the surface of a Zr anode after electrolysis at 50 V for 10 min in Br-ACE.

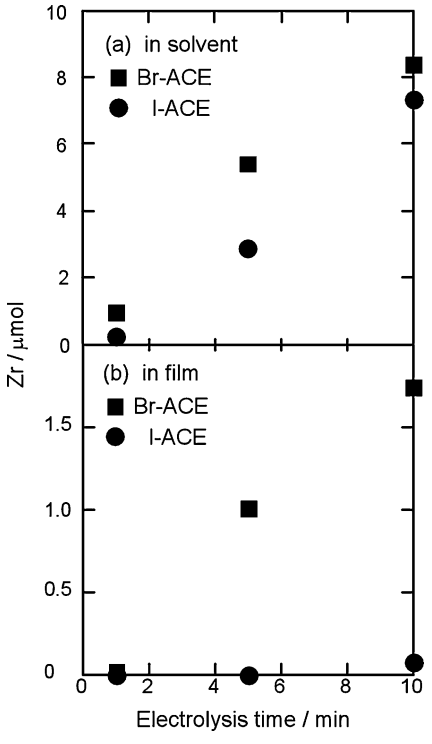

Figure 4 Amount of Zr in (a) solvent and (b) as-deposited films as measured by ICP spectroscopy as a function of electrolysis time under application of 5 mA current.

oxidation of Zr and film formation on the cathode in acetone without halogen additive under an applied electric field.

Halide ions in an electrolyte strongly promote anodic corrosion. The etching force for an anodic ZrO_2/Zr film decreases in the order $Cl^- > Br^- > I^-$ [20]. In the authors' previous study, the difference in corrosiveness between I^- and Br^- was distinctly revealed in the case of anodic dissolution of Ta and Nb in the same solvent. In these cases, anodic dissolution of M_2O_5/M proceeded only in Br-ACE, but not in I-ACE. These facts can be understood by the difference in durability of the metals with respect to halide ions, i.e. (Al, Zr, Ti) $\ll$ (Ta, Nb). Another group reported that Br^- ions form the strongest chemical bond with the outermost layer of oxide, strongly assisting in the potential-dependent chemical dissolution of the oxide film [23]. In addition, the ionic radius of aggressive halide ions may affect the dissolution rate of ZrO_2/Zr. That is, small bromide ions are able to infiltrate into the passive oxide film more readily than the larger iodine ions, thereby promoting dissolution of the metal substrate [24]. As a result, the deposition of Zr in the case of Br-ACE proceeds faster. Although the addition of hydrogen halide (HX) will give a similar result, gas-phase additives are difficult to handle for processing. Thus, I_2 or Br_2 are considered to be the most appropriated additives as an aggressive reagent for the present solvent.

As stated already, the ZrO_2/Zr layer dissolves due to the effect of halide ions, releasing zirconium species into the solvent. Consistent with reaction (2), the present halogenated acetone solvent has a high proton content. According to the literature [22], $[H^+]$ of I-ACE is estimated to be 2×10^{-4} M for 0.01 M I_2, as determined by neutralization titration. Therefore, ZrO^{2+} (zirconyl ion), which is a stabilized form in the acidic conditions, is considered to be released to the solvent as a result of anodic corrosion. If this ZrO^{2+} readily precipitates as polymeric zirconia and deposits electrophoretically on the cathode, the zeta potential of the solution would shift from nearly zero to positive in an acidic solution after electrolysis [25]. The zeta potentials of the solutions, however, did not change after electrolysis. This supports the idea that the zirconium species existed as an isolated ion state in the solution. We have already investigated the role of water in the present technique using Ta anode [18]. Although the Br-ACE contained a large amount of H_2O (2 M), anodic dissolution and cathodic deposition proceeded similarly to when the solvent did not contain additional H_2O (0.13 M). Judging from this result, it is thought that strict control of the electrolysis condition such as dehumidification of organic solvent or deposition in an inert atmosphere is not necessary. However, attempt to increase the H_2O content in Br-ACE (about 8 M) has led to the formation of powdery white deposits that has very weak adhesion to the cathode.

The following reaction for ZrO^{2+} may also proceed to yield $Zr(OH)_2^{2+}$ due to the influence of water present as an impurity in acetone [26].

$$ZrO^{2+} + H_2O \rightarrow Zr(OH)_2^{2+} \quad (3)$$

In this case, ZrO^{2+} and/or $Zr(OH)_2^{2+}$ diffuse in the cathodic direction to deposit electrochemically on the cathode surface. Hydrolysis of zirconium species with OH^- (as described by reactions (4) and (5) below) produced by the reduction of H_2O (6) and/or dissolved oxygen (7) results in the accumulation of a gel on the cathode surface [27–29].

$$ZrO^{2+} + H_2O + 2OH^- \rightarrow Zr(OH)_4 \quad (4)$$

$$Zr(OH)_2^{2+} + 2OH^- \rightarrow Zr(OH)_4 \quad (5)$$

$$2H_2O + 2e^- \rightarrow 2H_2 + 2OH^- \quad (6)$$

$$O_2 + 2H_2O + 4e^- \rightarrow 4OH^- \quad (7)$$

Fig. 5 shows EPMA elemental distribution maps for the Pt cathode surface after electrolysis using the Zr anode in I-ACE. At high voltage (50 V), platelet films with cracks are deposited on the entire surface. The crack development will depend mainly on the hydrogen gas evolution in accordance with reaction (4), and on volume shrinkage resulting from evaporation of solvent during drying. However, a uniform coating without structural defects is desired from the viewpoint of practical application. Such a smooth defect-free film was successfully obtained by electrolysis at 10 V for 10 min. TG/DTA of as-deposited film detected a major weight loss in each of the two temperature ranges (RT–723 K and 723–823 K), and the total loss up to 1473 K was about 35%. This is similar to that of zirconium hydroxide, which was electrochemically prepared in $ZrOCl_2$ aqueous solution [30]. The first decrease in the weight ($\sim$30%) appears to result from the

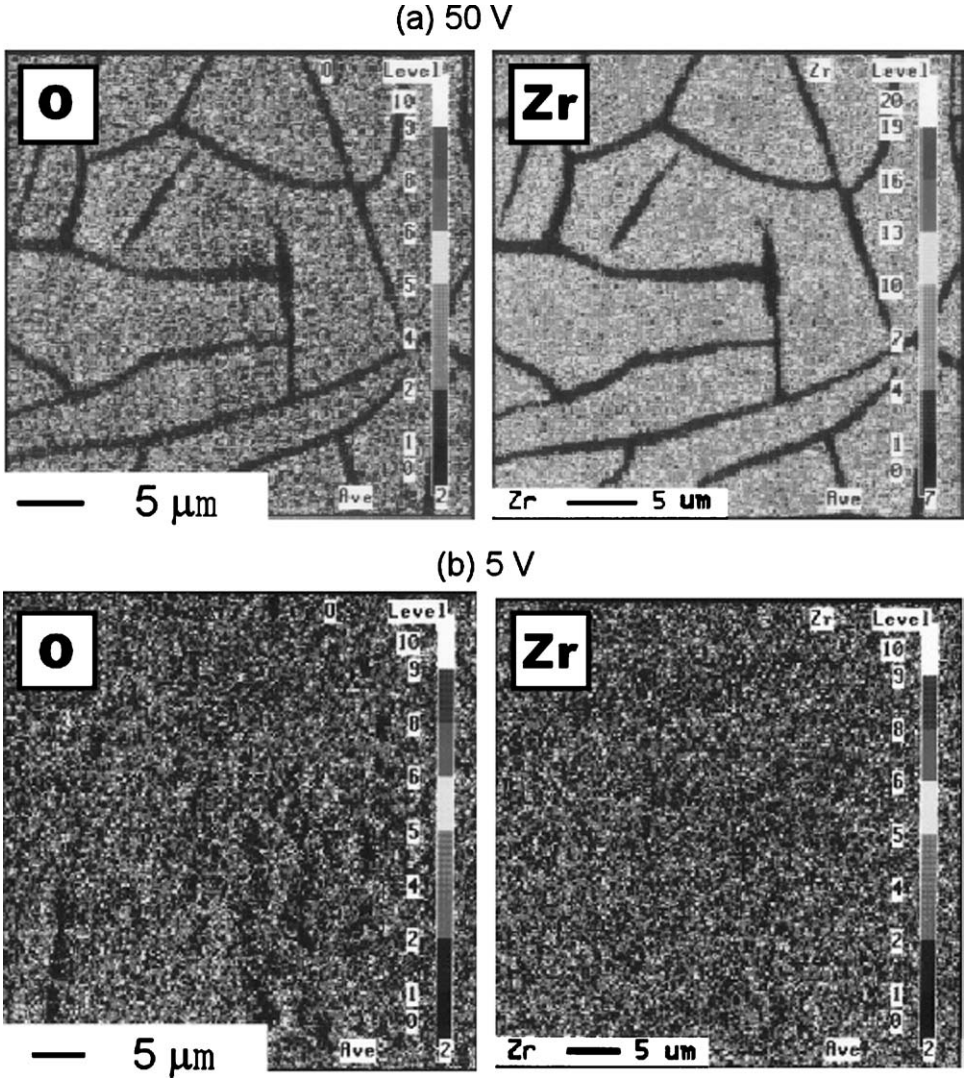

Figure 5 EPMA elemental distribution maps of the surface of films prepared at (a) 50 and (b) 10 V for 10 min.

evaporation of acetone and/or water remained in the film. In the second stage, the sudden loss (∼35%) with an exotherm is attributable to the dehydration of hydroxide or hydrated oxide. The exothermic peak is considered to be due to crystallization of zirconia phase. The crystal structures of deposited films before and after heat treatment were determined by analysis of XRD patterns measured at ambient temperature. As expected, the as-deposited film is amorphous, and becomes monoclinic ZrO_2 crystal upon thermal processing at 1273 K in air.

Fig. 6 shows the potentiodynamic polarization curve for the stainless steel substrate covered with $Zr(OH)_4$ film (50 V, 10 min in I-ACE) after annealing at 773 K for 60 min in 0.1 M KCl solution (pH 6.5). For comparison, this figure also shows the curve for an uncoated stainless steel substrate after annealing. The polarization curves of two substrates show Tafel-type behavior. The corrosion potential (E_{corr}) of the coated stainless steel substrate is shifted toward a more positive potential compared to the uncoated sample. Moreover, the corrosion current of the coated substrate was reduced by two orders of magnitude. These results indicate that the dense zirconia coating inhibits the permeation of aggressive ions (Cl^-) through the film [31], acting as an effective barrier against electrolytic corrosion [32]. Since the present electrochemical method is one of simple solution process, any electrically conductive substrate and/or complex shaped substrate are thought to be applicable for anti-corrosion coating.

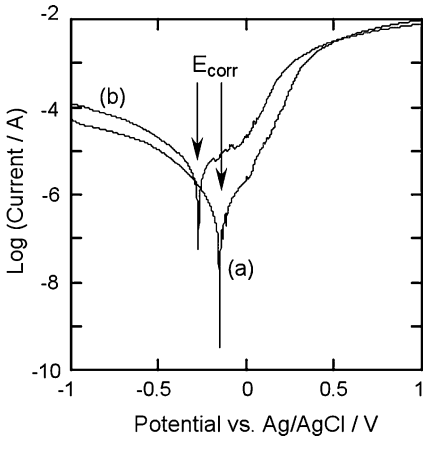

Figure 6 Potentiodynamic polarization curve of (a) zirconia-coated stainless steel substrate (50 V, 10 min) after annealing at 773 K for 1 h in 0.1 M KCl solution, and (b) uncoated stainless steel substrate after identical thermal treatment.

In conclusion, zirconium (IV) and aluminum (III) oxide films were successfully fabricated in an acetone bath containing conductive halide additives using a soluble Zr and Al anode as the metal source. The electrodeposition mechanism was resolved into three processes. First, anodic oxidation of the metal anode proceeds in the presence of water as an impurity in the acetone solvent. Subsequently, the oxide film on the metal anode undergoes pitting corrosion through reaction with the halide ions, and finally, the metal species produced by this corrosion are deposited directly onto the cathode surface through reaction with hydroxide ions generated at the cathode. In the present electrolysis mechanism, the corrosiveness of halogen additive was found to be a significant factor determining the deposition amount of metal species. That is, bromide ions are more aggressive for electrochemical dissolution of the metal anode compared to iodide ions. A stainless steel substrate coated with the zirconia film exhibited good protection against electrolytic corrosion.

Acknowledgement

The authors thank to the Tokuyama Science Foundation for financial support.

References

1. P.-F. CHAUVY, P. HOFFMANN and D. LANDOLT, *Electrochem. Solid-State Lett.* **4** (2001) C31.
2. E. A. PONOMAREV and C. LÈVY-CLÈMENT, *ibid.* **1** (1998) 42.
3. Y. C. WANG, I. C. LEU and M. H. HON, *J. Mater. Chem.* **12** (2002) 2439.
4. *Idem.*, *Electrochem. Solid-State Lett.* **5** (2002) C53.
5. Y. ISHIKAWA and Y. MATSUMOTO, *Solid State Ionics* **151** (2002) 213.
6. Y. MATSUMOTO, Y. ISHIKAWA, M. NISHIDA and S. II, *J. Phys. Chem.* B **104** (2000) 4204.
7. T. SUGIURA, T. YOSHIDA and H. MINOURA, *Electrochem. Solid-State Lett.* **1** (1998) 175.
8. M. T. REETZ and W. HELBIG, *J. Amer. Chem. Soc.* **116** (1994) 7401.
9. M. T. REETZ, S. A. QUAISER and C. MERK, *Chem. Ber.* **129** (1996) 741.
10. S. SHIMADA and M. HASEGAWA, *J. Amer. Ceram. Soc.* **86** (2003) 177.
11. L. E. GRIFFITHS, M. R. LEE, A. R. MOUNT, H. KONDOH, T. OHTA and C. R. PULHAM, *Chem. Comm.* (2001) 579.
12. K. KAMADA, M. MUKAI and Y. MATSUMOTO, *Electrochim. Acta* **47** (2002) 3309.
13. L. ARIES, L. ALBERICH, J. ROY and J. SOTOUL, *ibid.* **41** (1996) 2799.
14. P. J. MITCHELL, R. J. MORTIMER and A. WALLACE, *J. Chem. Soc. Faraday Trans.* **94** (1998) 2423.
15. T. ISHIHARA, K. SATO, Y. MIZUHARA and Y. TAKITA, *Chem. Lett.* (1992) 943.
16. Y. MATSUMOTO, H. ADACHI and J. HOMBO, *J. Amer. Ceram. Soc.* **76** (1993) 769.
17. A. MUKHERJEE, D. HARRISON and E. J. PODLAHA, *Electrochem. Solid-State Lett.* **4** (2001) D5.
18. K. KAMADA, M. MUKAI and Y. MATSUMOTO, *Electrochim. Acta* **49** (2004) 321.
19. P. STEFANOV, D. STOYCHEV, I. VALOV, A. KAKANAKOVA-GEORGIEVA and T. S. MARINOVA, *Mater. Chem. Phys.* **65** (2000) 222.
20. G. A. EL-MAHDY, S. S. MAHMOUD and H. A. EL-DAHAN, *Thin Solid Films* **286** (1996) 289.
21. T. TSUKADA, S. VENIGALLA and J. H. ADAIR, *J. Amer. Ceram. Soc.* **80** (1997) 3187.
22. Y. TAKAYAMA, H. NEGISHI, S. NAKAMURA, N. KOURA, Y. IDEMOTO and F. YAMAGUCHI, *J. Ceram. Soc. Jpn.* **107** (1999) 119.
23. S. B. BASAME and H. S. WHITE, *J. Electrochem. Soc.* **147** (2000) 1376.
24. F. H. ASSAF, S. S. ABD EL-REHIEM and A. M. ZAKY, *Mater. Chem. Phys.* **58** (1999) 58.
25. I. ZHITOMIRSKY and A. PETRIC, *Mater. Lett.* **46** (2000) 1.
26. K. NAKAJIMA, S. SHIMADA and M. INAGAKI, *J. Mater. Chem.* **6** (1996) 1795.
27. M. KOINUMA, H. OHMURA, Y. FUJIOKA, Y. MATSUMOTO and S. YAMADA, *J. Solid State Chem.* **136** (1998) 293.
28. P. STEFANOV, D. STOYCHEV, M. STOYCHEVA, J. IKONOMOV and T. S. MARINOVA, *Surf. Interf. Anal.* **30** (2000) 628.
29. I. ZHITOMIRSKY and A. PETRIC, *Mater. Lett.* **50** (2001) 189.
30. I. ZHITOMIRSKY and L. GAL-OR, *J. Mater. Sci.* **33** (1998) 699.
31. G. P. THIM, M. A. S. OLIVEIRA, E. D. A. OLIVEIRA and F. C. L. MELO, *J. Non-Cryst. Solids* **273** (2000) 124.
32. Y. CASTRO, A. DURAN, R. MORENO and B. FERRARI, *Adv. Mater.* **14** (2002) 505.

Received 16 July 2003
and accepted 30 April 2004